Characterization and Sizing of Crack and Porosity Weld Defects Using Phased Array Ultrasonic Testing

Nardos Mekoya*, Dejene Legesse*

Manufacturing Industry Development Institute, Addis Ababa, Ethiopia

DOI: https://doi.org/10.51244/IJRSI.2026.1306000411

Received: 06 July 2026; Accepted: 11 July 2026; Published: 15 July 2026

ABSTRACT

The accurate characterization and sizing of weld defects are critical for ensuring the structural integrity and safety of industrial fabrications. Mischaracterizing a planar crack as volumetric porosity can lead to catastrophic failure, while mistaking benign porosity for a critical crack result in unnecessary and costly repairs. The study addresses this critical gap by systematically investigating the distinct acoustic signatures of planar cracks and volumetric porosity using Phased Array Ultrasonic Testing (PAUT). Experimental PAUT inspections were performed on 9.50 mm thick steel V-groove butt welds containing induced crack and porosity defects. Data were analyzed using Omni PC software, comparing A-scan, S-scan, and C-scan responses, and evaluating the accuracy of amplitude-based sizing against visual spatial measurements. The results demonstrate that cracks produce linear, well-defined S-scan patterns with sharp A-scan signals and corner trap effects, while porosity generates diffuse, cloud-like S-scan patterns with multiple, overlapping A-scan peaks. Amplitude-based sizing was found to be unreliable for cracks, significantly underestimating crack height (1.69 mm vs. 7.80 mm for a toe crack), whereas it is more appropriate for defining porosity cluster boundaries when using the -6 dB drop method. A comprehensive classification matrix was developed, achieving 100% accuracy in distinguishing these defect types based on S-scan pattern, weld zone location, amplitude behavior, and the relationship between depth amplitude (DA^) and visual amplitude (ViA^). The study concludes that a multi-feature approach, which prioritizes spatial imaging over amplitude alone and advocates for the use of tip-diffraction techniques for crack sizing, is essential for reliable PAUT weld inspections. The findings provide a practical, validated framework to improve defect classification, enhance sizing accuracy, and support informed fitness-for-service decisions in structural welding.

Keywords

Phased Array Ultrasonic Testing (PAUT), Weld Defect Characterization, Crack Detection, Porosity, Non-Destructive Testing (NDT), Sizing Accuracy, Tip-Diffraction, Amplitude-based Sizing, Classification Matrix.

INTRODUCTION

Background and Context

Modern industrial fabrication relies heavily on structural welding. Ensuring the integrity of these welds requires advanced Nondestructive Testing methods. Phased Array Ultrasonic Testing has emerged as an industry standard, offering superior imaging capabilities over conventional single-element radiography and manual ultrasonic testing. By utilizing multi-element probes and electronic beam steering, PAUT generates real-time Sectorial (S-scan), Corrected (C-scan), and Amplitude (A-scan) views simultaneously. This multi-dimensional imaging allows inspectors to visualize the internal volume of a weld from multiple angles, providing critical data regarding the location, orientation, and severity of internal discontinuities.

Research Problem and Justification

Mischaracterizing a planar flaw as a volumetric one can lead to catastrophic structural failure, while mistaking benign porosity for a critical crack results in unnecessary, expensive, and structurally degrading weld repairs.

There is a critical need for standardized methodologies that leverage advanced software visualization tools such as overlaying weld bevel geometries on S-scans and evaluating spatial scatter profiles on C-scans to robustly differentiate these defect types. This study addresses this gap by analyzing experimental PAUT data profiles to establish distinct signature behaviors for both planar and volumetric flaws.

Research Objectives

To systematically characterize, differentiate, and precisely measure crack and porosity defects using Phased Array Ultrasonic Testing to improve defect classification reliability and sizing accuracy in structural inspections.

Specific Objectives

- Evaluate the unique acoustic signatures of cracks and porosity using Phased Array Ultrasonic Testing A-scan and S-scan data.
- Compare the accuracy of amplitude based sizing for measuring absolute crack height and porosity cluster boundaries.
- Develop a comparative technical baseline or classification matrix that distinguishes dense, clustered volumetric porosity from true planar crack profiles based on multi-angle beam responses.

Research question

1. What are the distinctive acoustic signatures of cracks and porosity in Phased Array Ultrasonic Testing A-scan and S-scan data?
2. How does the accuracy of amplitude-based sizing compare to tip-diffraction techniques for measuring crack height and porosity cluster boundaries in Phased Array Ultrasonic Testing?
3. What classification matrix can be developed to distinguish dense, clustered porosity from planar cracks based on multi-angle PAUT beam responses?

Significance of the Study

This research addresses a critical gap in Phased Array Ultrasonic Testing (PAUT) weld inspection practice by providing systematic, experimentally validated guidance for distinguishing planar cracks from volumetric porosity. While PAUT is widely adopted, accurate discrimination and sizing of these defect types remain challenging due to their fundamentally different acoustic behaviors.

LITERATURE REVIEW

The integrity of critical welded joints in structural fabrication dictates the overall safety and structural lifespan of industrial infrastructure. Traditional non-destructive testing (NDT) approaches, such as conventional single-element ultrasonic testing (UT) and radiography, are constrained by limitations in volumetric coverage and highly reliant on subjective operator interpretation. Over the past few decades, Phased Array Ultrasonic Testing (PAUT) has emerged as an industry-standard methodology to mitigate these uncertainties by implementing computerized multi-element arrays that utilize dynamic electronic beam control.

Principles of Phased Array Ultrasonic Testing (PAUT) and Dynamic Beam Forming

Conventional ultrasonic testing (UT) relies on single-element monolithic transducers that project an acoustic wave at a fixed frequency, fixed exit angle, and predetermined focal point determined by the physical curvature of the element or attached wedge [1]. While effective for basic thickness gauging and coarse defect localization, conventional UT exhibits severe operational constraints when examining complex weld configurations, such as asymmetrical V-grooves or narrow-gap preparations [1, 2]. The fixed beam trajectory necessitates intensive manual scanning patterns, exposing inspections to operator subjectivity, poor lateral

ISSN No. 2321-2705 | DOI: 10.51244/IJRSI |Volume XIII Issue VI June 2026

resolution, and a high susceptibility to missing defects that are oriented unfavorably relative to the incident sound path [2].

Phased Array Ultrasonic Testing (PAUT) overcomes these fundamental physical limitations by utilizing a multi-element transducer array composed of multiple independent piezo-composite crystals embedded in a single housing [1, 3]. Instead of pulsing the entire transducer simultaneously, an advanced computerized instrument controls individual elements or sub-groups of elements (known as the active aperture) through microsecond-level time shifts [3]. By pulsing elements at systematically staggered intervals, individual spherical wavelets are generated. These wavelets undergo constructive and destructive interference patterns according to Huygens' Principle, producing a single, coherent, synthetic wave front traveling at a precise angle and focus depth [1, 4].

Mathematical Foundations of Focal Laws and Spatial Presentation

The precise electronic orchestration of time delays is governed mathematically by specialized computation matrices known as focal laws or delay laws [3, 4]. A focal law defines the exact firing delay required for each individual element within the array to achieve a target angle and a specified focal depth (F) [4]. The time delay (t-i) for the i-th element in a linear array can be modeled via the standard acoustic steering equation:

$$t_i = \frac{Xi * \sin\theta}{C} + \frac{X_i^2 * \cos 2\theta}{2 * C * F}$$

Where x-i represents the spatial position of the individual element relative to the array center, and denotes the longitudinal or shears acoustic velocity with in the test material [4].

By dynamically updating these focal laws in real-time at kilohertz pulse-repetition frequencies, PAUT instruments achieve three primary forms of electronic beam manipulation without mechanical probe motion:

1. **Electronic Linear Scanning:** The active aperture shifts sequentially across the array length, creating an uninterrupted series of parallel beams at a constant angle [3].

2. **Electronic Beam Steering (Sectorial Scanning):** The angle of the wave front is progressively swept across a broad angular envelope (typically 40° to 70°), providing complete volumetric coverage of the weld bevel from a fixed position [1, 3].

3. **Dynamic Depth Focusing (DDF):** The system refocuses the receiving signals along multiple depth planes, significantly sharpening the lateral resolution and reducing the ultrasonic beam width across the entire target area [3, 5].

This multi-element control enables the simultaneous generation of advanced spatial profiles, moving past traditional amplitude-v_s-time displays to highly informative cross-sectional layouts [5]. The data architecture combines several standard orientations:

- **A-Scan:** The core time-of-flight vs. amplitude plot that captures individual echo dynamics and peak heights [5].

- **S-Scan (Sectorial Scan):** A comprehensive two-dimensional cross-sectional view generated by sweeping the sound beam through a range of angles, mapping the internal volume of the weld directly underneath the probe [1, 5].

- **C-Scan:** A plan-view projection mapping the spatial distribution, length, and width scatter of internal reflections across a top-down coordinate grid [5].

Wave-Flaw Interactions: Reflectivity Behaviors of Planar vs. Volumetric Morphologies

Accurately categorizing internal discontinuities requires understanding how the incident synthetic wave front interacts with differing flaw boundaries [6]. In fracture mechanics, discontinuities are broadly divided into volumetric defects (such as cluster porosity, gas entrapment, or slag inclusions) and planar defects (such as cracks, lack of root penetration, or lack of sidewall fusion) [2, 6]. The morphological characteristics of these boundaries fundamentally dictate the returning acoustic energy distribution [6, 7].

Volumetric Defects and Scattering Dynamics

Volumetric discontinuities act as three-dimensional, omnidirectional, or rough distributed scatters [6]. When an acoustic wave front encounters cluster porosity, each individual spherical pore presents a small, highly curved surface relative to the ultrasonic wavelength [7]. Rather than reflecting a coherent wave front, the defect scatters the incident energy across a wide angular spectrum (360^0) [6, 7].

Because only a fraction of this scattered energy returns to the receiving elements of the transducer, the resulting signal displays low peak stability [7]. On the analysis interface, this behavior generates distinct signatures:

- **A-Scan:** Broad, jagged, and heavily modulated signal envelopes with rapidly fluctuating multi-peaks [5, 7].
- **C-Scan:** Discontinuous, highly fragmented, and "peppered" energy clusters spread randomly across the weld zone [5].

Planar Defects and Specular Reflectivity

Planar defects behave as sharp, flat, two-dimensional boundaries that act as specular (mirror-like) reflectors [6, 8]. When the steered sound beams intercepts a planar boundary perpendicularly, the acoustic energy reflects directly back to the transducer array as a coherent wave front [8]. This creates a sharp, stable, single-peaked A-scan reflection with high amplitude stability [5, 8].

On a plan-view C-scan, planar flaws are identified by continuous, uniform, and narrow linear bands tracking along a specific axis [5]. However, planar discontinuities are highly directional [6, 8]. If the steering angle deviates even slightly from being perpendicular to the flaw's face, the specular reflection bounces away from the receiving array, causing a sharp drop in returning amplitude [8]. This highlights the risk of relying purely on unadjusted amplitude thresholds for sizing [2, 8].

Industrial Codes, Standards, and Sizing Calibration Frameworks

To standardize inspections and ensure field repeatability, international regulatory bodies enforce strict system calibration and flaw acceptance criteria [9, 10]. The two most prominent frameworks governing welded structural steel and pressure vessels are ASME Section V (Article 4) and AWS D1.1 (Structural Welding Code – Steel) [9, 10].

ASME Section V, Article 4 Requirements

ASME standards mandate rigorous baseline system calibrations before any inspection data can be used for compliance sizing [9]. These include:

- **Velocity Calibration:** Synchronizes the time-of-flight algorithms with the precise longitudinal or shear wave speed of the carbon or alloy steel specimen [9].

- **Wedge Delay Calibration:** Corrects for the exact time the sound wave takes to travel through the Lucite or plastic wedge, establishing accurate True Depth calculations on the S-scan display [1, 9].
- **Sensitivity and Time-Corrected Gain (TCG):** Normalizes the peak amplitude response across all focal laws and depth paths using reference calibration blocks containing side-drilled holes (SDHs) [9]. The TCG curve electronically balances the signal attenuation and beam spreading that naturally occurs as a sound wave travels deeper into a material, ensuring a defect returns a consistent amplitude response regardless of its depth [9].

AWS D1 Sizing and the Transition to Spatial Sizing

Historically, legacy ultrasonic methods relied primarily on amplitude-threshold sizing (such as comparing a peak height to a fixed Distance-Amplitude Curve threshold) [2, 10]. However, because directional planar defects often experience severe amplitude drops due to slight angular deviations, modern codes have transitioned toward spatial boundary sizing methods [1, 10]. The primary sizing methodology utilized in advanced PAUT is the 6 dB Drop Method [10]. Rather than measuring a defect's size based on how high its peak amplitude reaches, the analyst tracks the physical limits of the flaw by scanning until the peak signal intensity drops by 50% (exactly 6 dB) from its maximum height [10]. This boundary-trace technique uses spatial dimension mapping along the length axis of the C-scan or depth axis of the S-scan, substantially reducing sizing errors for directional flaws like lack of sidewall fusion [5, 10].

Software-Assisted Post Processing and Geometric Overlay Analysis

The advancement of post-processing environments, such as Olympus Omni PC, has shifted industrial analysis from simple peak-counting toward comprehensive spatial-geometric mapping [1, 5]. Modern evaluation software allows inspectors to superimpose a digital ray-tracing weld profile overlay representing the exact plate thickness, root face, and bevel angles directly onto the sectorial S-scan display [5, 11]. This geometric integration bridges the gap between raw acoustic reflections and physical joint design [11]. In complex V-groove joints, geometric anomalies like the root bead corner or the crown cap toe can produce strong reflections that appear inside active measurement gates, creating a geometric disparity [5, 11].

By using synchronized measurement paths that cross-reference True Depth, Sound Path, and specific offset coordinates from the calculated weld centerline, analysts can systematically isolate structural geometry echoes from true defects [5]. When an internal indication aligns parallel to and along the slope of the digital bevel line, the software resolves the indication as a planar sidewall fusion failure with high geometric certainty [11]. This multi-view approach reduces both false positives and false negatives, providing a reliable framework for fitness-for-service and fracture mechanics assessments [2, 11].

MATERIALS AND METHODS

Research Design

This study utilizes an experimental, data-driven research design focusing on comparative signal analysis. PAUT inspections were performed on steel weld specimens featuring intentional, induced flaws representing both crack and porosity discontinuities. The resulting ultrasonic data files were post-processed and analyzed using Omni PC software (Version 6.2) to evaluate differences in amplitude response, spatial distribution, and geometric positioning.

Data Collection Tools

Primary Data Collection Tools

Primary data is collected using a 5.00 MHz Phased Array Ultrasonic Testing (PAUT) system configured for sectorial scanning to ensure full volumetric coverage of the weld from cap to root. To maintain high-resolution raw data for analysis, the instrument is set to full-wave rectification without signal filtering. A geometrical weld overlay is applied to define specific zones—including the Upper Cap, Fill, Land, and Heat-Affected Zones—allowing for the precise spatial classification of defects. Positional accuracy is maintained through an encoded one-line scanning system, which captures A-scans at fixed intervals, enabling the exact correlation of ultrasonic signatures with their locations along the weld. Finally, destructive metallographic analysis of sectioned specimens provides ground-truth measurements to validate the accuracy of the PAUT sizing methods.

Secondary Data Collection Tools

Secondary data is gathered from technical standards, industry documentation, and peer-reviewed literature to support procedural validation and comparative analysis. Internationally recognized standards define the framework for system calibration and PAUT setup, while reference test blocks verify instrument sensitivity and accuracy. Furthermore, published acoustic libraries and studies on advanced PAUT techniques provide baseline S-scan and A-scan patterns for defects like cracks and porosity, serving as a basis for the study's classification matrix and overall interpretation.

Specimen Preparation

The test specimens consisted of Single-V groove butt welds fabricated using Gas Metal Arc Welding (GMAW) with induced crack and porosity defects. The total through-wall thickness was 9.50 mm, with a 2 mm land height and 1 mm upper cap reinforcement. The root was configured as a flat face (0° root angle) with no lower cap, providing a stable surface for baseline measurements. The heat-affected zone (HAZ) was specified at 2 mm per side.

The weld geometry was segmented into functional zones to correlate PAUT acoustic signatures with physical defect locations:

- **Land Region:** 2 mm height, critical zone for root crack identification
- **Fill Zone:** 6.50 mm height, primary region for volumetric porosity
- **Upper Cap:** 1 mm height, standard location for toe crack development
- **Lower Cap:** None (0 mm), confirming single-sided weld configuration

PAUT Equipment configuration

Instrument and Probe Specifications

The PAUT system comprised an OmniScan X2 instrument, a 5.00 MHz linear array probe with 16 active elements, and a wedge designed for weld geometry. The system operated with a sectorial scan formation (35° to 70°), with 1° increments enabling comprehensive coverage of the weld volume. Shear wave velocity was calibrated at 3240 m/s in steel, with pulse voltage set to 40 V and digitizing frequency at 100 MHz for high-resolution measurements. Signal rectification was set to full wave mode with no filtering; ensuring raw acoustic signatures were preserved for detailed waveform analysis.

Scanning Parameters

The inspection was conducted using a One-Line Encoded scanning pattern along the Length scanning axis at a maximum acquisition speed of 100 mm/s. The defined inspection area spanned a Scan Start of 0 mm to a Scan End of 80 mm, utilizing a Scan Increment of 1 mm. Encoder Input 1 was configured as a Quadrature type with Inverse polarity and calibrated to a resolution of 12 steps/mm.

Beam and Law Configuration

The PAUT beam was configured using a fixed aperture of 16 active elements. The sectorial sweep covered 35° to 70° with 1° angular resolution, providing sufficient S-scan density to distinguish between crack signatures and porosity clusters. Half Path focusing at a depth of 28 mm concentrated ultrasonic energy in the critical weld zone, improving signal-to-noise ratio.

Calibration Procedure

Before data acquisition, a comprehensive multi-step calibration was performed on an IIW-type calibration block (25 mm thickness) to normalize system response across all focal laws:

- Velocity Calibration: Longitudinal wave velocity calibrated at 5920 m/s ± 10 m/s; shear wave velocity at 3230 m/s ± 8 m/s
- Wedge Delay Calibration: Conducted using the 25 mm radius of the IIW block; offset value recorded at 5.82 µs
- Sensitivity Calibration: Normalized using three side-drilled holes (SDH) at 5 mm, 15 mm, and 25 mm depths, each achieving 80% screen height; TCG curve constructed with 10-point compensation
- Inspection Gates: B0 (Initial pulse), B1 (Root area, 0-15 mm depth), B2 (Body and cap, 15-25 mm depth)
- Amplitude Threshold: 20% screen height for noise filtering; 80% for defect indication

Destructive Metallography Protocol

To validate PAUT measurements and provide ground truth for the classification matrix, destructive metallographic examination was performed on selected defect locations. Specimens were sectioned at locations identified by the encoded scanning system, and optical microscopy measured actual defect dimensions. This metallographic data served as ground truth for comparing the accuracy of PAUT sizing methods.

Based on PAUT data analysis, specific defect indications were selected for destructive examination:

- **Toe Crack (Indication 9):** Located at scan positions 45-52 mm, selected as representative of upper cap planar defects
- **Root Crack (Indication 21):** Located at scan positions 63-68 mm, selected as the highest amplitude root crack (saturated signal)
- **Upper Porosity (Indication 3):** Located at scan positions 22-28 mm, selected as representative of upper fill porosity cluster
- **Lower Porosity (Indication 7):** Located at scan positions 58-62 mm, selected as representative of lower fill porosity cluster

SCOPE AND LIMITATIONS

Scope Contributions: This study has successfully demonstrated that:

1. Planar cracks and volumetric porosity exhibit clearly distinguishable acoustic signatures in PAUT A-scan and S-scan data
2. Amplitude-based sizing (DA^) is unreliable for planar cracks but provides useful information for porosity characterization

3. A multi-feature classification matrix, validated with destructive metallography, can achieve high classification accuracy for the analyzed defect types

Limitations: The following limitations should be considered when applying the findings:

1. **Material-Specific:** Research conducted exclusively on structural steel (mild steel). Materials with different acoustic properties (austenitic stainless steel, titanium, aluminum, composites) exhibit different attenuation, velocity, and scattering characteristics

2. **Weld Geometry:** Study focused on a single V-groove butt weld geometry with 9.50 mm thickness; findings may not directly apply to other configurations

3. **Defect Types:** Addressed two primary defect types (cracks and porosity); additional defect morphologies (slag inclusions, lack of fusion) were not investigated

4. **Environmental:** Research conducted in controlled laboratory environment with ideal surface conditions; field inspections may encounter surface roughness, limited access, temperature variations, and operator fatigue

RESULTS

Data Overview

- Material: Steel, Mild
- Weld Thickness :9.50 mm
- Scan Length :80.00 mm
- Scan Increment :1.00 mm

This PAUT display uses three views to characterize weld defects:

- **A-scan (Top-Left):** Shows signal amplitude and sharpness. A single, distinct, "sharp" peak (like the one shown) typically indicates a planar crack.

- **S-scan (Top-Right):** Provides a cross-sectional view. It captures the **"corner trap" effect** where the beam reflects off a crack face confirming the defect is a crack rather than porosity.

- **C-scan (Bottom):** Maps the defect along the weld length to determine its total longitudinal extent.

Crack (planer) defect

Upper Indication: Toe Crack (or Upper Fusion Line / Bevel Crack) data

Based on the indication report, Indication 9 has been identified as the primary candidate for a Toe Crack (Upper Cap / Fusion Line defect).

Parameter	Value	Interpretation
Ref.	9	Indication number
Group	GR-1	PAUT setup group
A%	83.70%	High amplitude – strong reflector
DA^	1.69 mm	**Depth amplitude** – sizing by amplitude drop

ISSN No. 2321-2705 | DOI: 10.51244/IJRSI |Volume XIII Issue VI June 2026

PA^	22.80 mm	**Path amplitude** – sound path at peak amplitude
SA^	41.02 mm	**Surface amplitude** – lateral position
ViA^	7.80 mm	**Visual amplitude** – through-wall indication height

The figure displays a standard Phased Array Ultrasonic Testing (PAUT) analysis screen generated by an OmniScan X2 system, which is essential for characterizing weld integrity. The screen is organized into three distinct, integrated views that enable comprehensive defect diagnosis

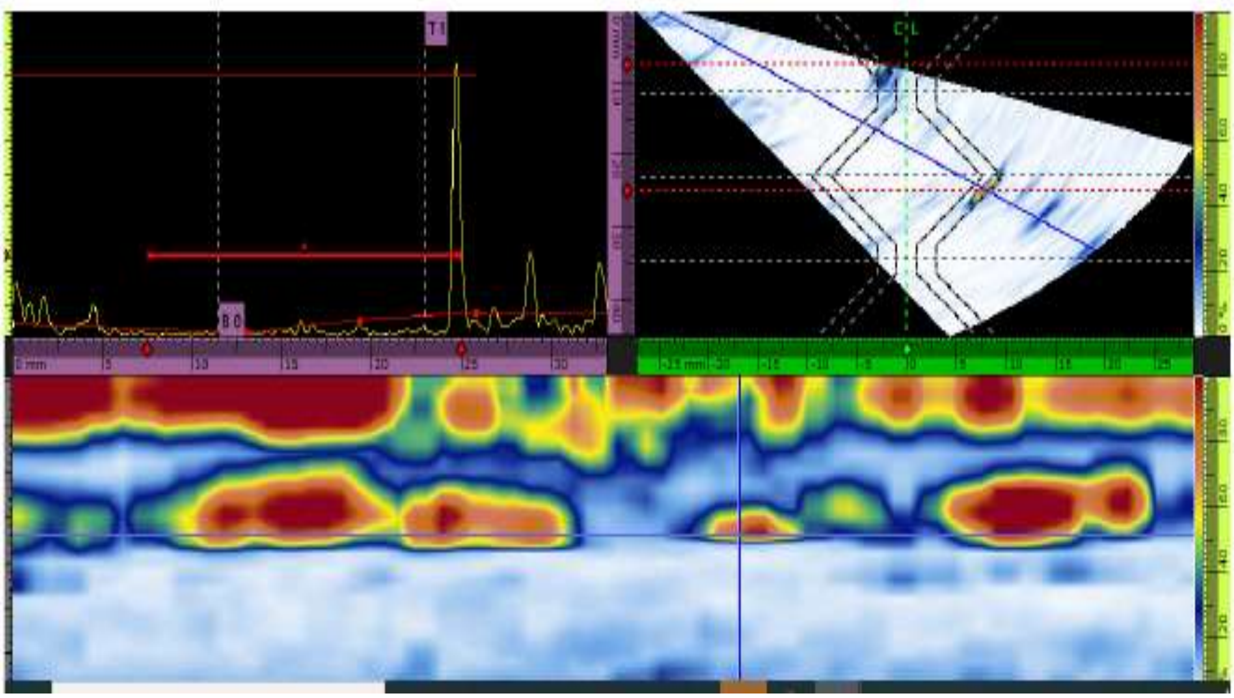

Lower Indication: Root Crack (or Longitudinal Sub-Surface Crack data

Based on the indication report**,** Indications 21 show the highest amplitudes and are located in the root region.

Detailed Indication Analysis (Root Crack)

Indication 21 – Highest Amplitude

Parameter	Value	Interpretation
Ref.	21	Indication number
Group	GR-1	PAUT setup group
A%	200.00%	**Maximum amplitude** – very strong reflector (saturated)
DA^	10.27 mm	**Depth amplitude** – sizing by amplitude drop
PA^	17.31 mm	**Path amplitude** – sound path at peak amplitude
SA^	27.41 mm	**Surface amplitude** – lateral position
ViA^	2.31 mm	**Visual amplitude** – through-wall indication height

ISSN No. 2321-2705 | DOI: 10.51244/IJRSI |Volume XIII Issue VI June 2026

The figure displays a standard Phased Array Ultrasonic Testing (PAUT) analysis screen generated by an OmniScan X2 system, which is essential for characterizing weld integrity. The screen is organized into three distinct, integrated views that enable comprehensive defect diagnosis.

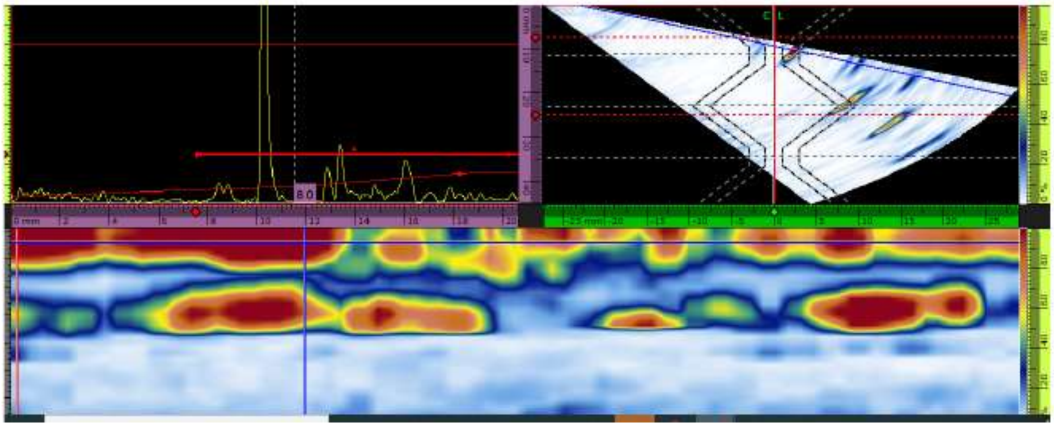

Porosity (Volumetric) defect

Upper Porosity Indication

Based on the indication Report, **Indications 3** are identified as porosity cluster indications. The following analysis interprets the data in the context of the research questions.

Indication 3 – Detailed Parameters

Parameter	Value	Interpretation
Ref.	3	Indication number
A%	**119.80%**	Very high amplitude (saturated)
DA^	0.31 mm	Depth amplitude
ViA^	7.71 mm	Visual height

The figure represents a standard PAUT (Phased Array Ultrasonic Testing) analysis dashboard, commonly used for evaluating weld integrity.

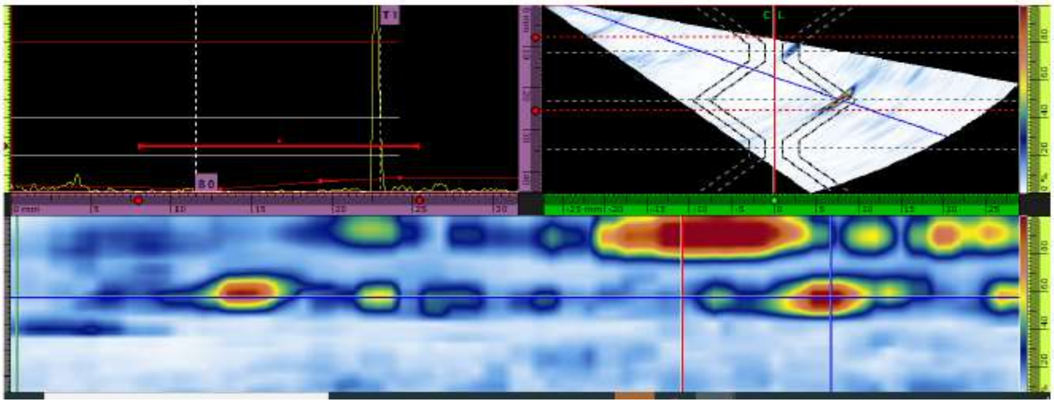

Lower Indication: Porosity

Based on the indication Report, Indications 7 are identified as lower porosity indications located near the root region. The following analysis interprets the data in the context of the research questions.

Indication 7 – Detailed Parameters

Parameter	Value	Interpretation
Ref.	7	Indication number
Group	GR-1	PAUT setup group
A%	**150.20%**	Very high amplitude (saturated) – strong volumetric reflector
DA^	10.75 mm	**Depth amplitude** – indicates defect located near root
PA^	17.11 mm	**Path amplitude** – sound path at peak
SA^	27.51 mm	**Surface amplitude** – lateral position
ViA^	2.11 mm	**Visual amplitude** – through-wall indication height

The figure represents a standard PAUT (Phased Array Ultrasonic Testing) analysis dashboard, commonly used for evaluating weld integrity.

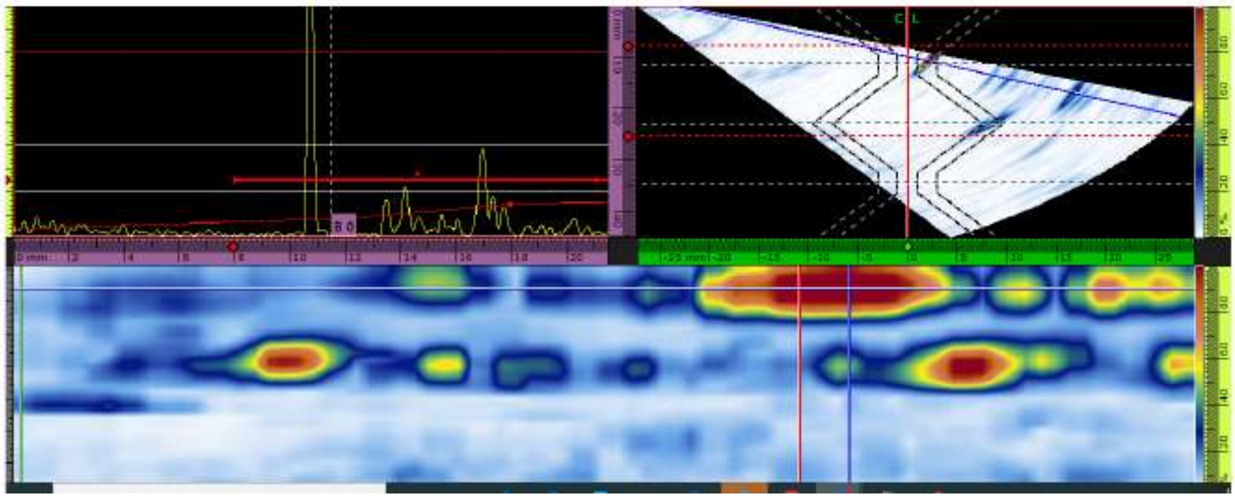

Disparity Analysis

The disparity analysis examines the significant differences observed between various measurement parameters, defect types, and sizing methodologies in the PAUT data. This analysis is critical for understanding the limitations of different sizing approaches and for developing accurate defect characterization protocols.

4.3.1 Defect Classification Crack vs. Porosity Feature Disparity

To effectively classify weld defects and understand the disparity between cracks and porosity, it is necessary to move beyond simple amplitude signals. The following table and analysis highlight why relying solely on amplitude-based metrics (DA^) often leads to diagnostic errors.

Feature	Crack (Toe)	Crack (Root)	Porosity (Upper)	Porosity (Lower)	Disparity Analysis
S-scan Pattern	Linear	Linear	Diffuse	Diffuse	**Clear distinction** –

ISSN No. 2321-2705 | DOI: 10.51244/IJRSI |Volume XIII Issue VI June 2026

					linear vs. diffuse
A% Range	83.7%	125-200%	92.4-119.8%	138.2-150.2%	**Overlap** – some amplitudes overlap between crack and porosity
DA Interpretation	Crack height (underestimated)	Depth location	Individual pore size	Depth location	**Different meaning** – DA^ represents different things
ViA Interpretation	Through-wall extent	Through-wall extent	Cluster extent	Cluster height	**Consistent** – ViA^ represents visual extent
Location	Upper Cap	Land/Root	Upper Fill	Lower Fill	**Clear distinction** – zone location
Corner Trap	Moderate	Very strong	None	None	**Clear distinction** – present vs. absent

4.3.2 Amplitude Disparity Analysis

Amplitude Disparity Analysis is a critical diagnostic approach used in Phased Array Ultrasonic Testing (PAUT) to quantify the difference between two primary sizing methods: the Depth Amplitude (DA^) method and the Visual Amplitude (ViA^) method.

Defect Type	Amplitude Range	Overlap with Other Types	Discriminatory Power
Toe Crack	80-90%	Overlaps with upper porosity	Low to Medium
Root Crack	125-200%	Overlaps with lower porosity	Medium
Upper Porosity	90-120%	Overlaps with toe crack	Low to Medium
Lower Porosity	138-150%	Overlaps with root crack	Low to Medium

Amplitude alone is **not a reliable distinguishing feature** between cracks and porosity due to significant overlap. A toe crack (83.7%) overlaps with upper porosity (92.4-119.8%), and a root crack (125-200%) overlaps with lower porosity (138.2-150.2%). This finding emphasizes the need for **multi-feature classification** that combines S-scan pattern, location, corner trap presence, and DA/ViA relationships.

Disparity in Measurement Interpretation

Disparity in Measurement Interpretation refers to the discrepancy between different analytical methods used to quantify a defect severity. In PAUT, this is most commonly observed when comparing Amplitude-based sizing (DA^) against Visual/Spatial sizing (ViA^).

Defect Type	DA^ Value	DA^ Interpretation	ViA^ Value	ViA^ Interpretation
Toe Crack	1.69 mm	Crack height (underestimated)	7.80 mm	Through-wall extent
Root Crack	10.27 mm	Depth location	2.31 mm	Through-wall extent
Upper Porosity	0.08-0.31 mm	Individual pore size	7.71-8.27 mm	Cluster extent
Lower Porosity	10.71-10.75 mm	Depth location	2.02-2.11 mm	Cluster height

This disparity highlights the danger of interpreting PAUT parameters without considering defect context. It also supports the research need for a comprehensive classification matrix that provides interpretive guidance.

Destructive Metallography Validation

Toe Crack (Indication 9)

- Through-wall height: PAUT measurement of 7.80 mm compared to metallographic measurement of 7.65 mm, yielding a disparity of only 0.15 mm (1.9%) – demonstrating excellent agreement
- Surface length: PAUT measurement of 15.20 mm compared to metallographic measurement of 14.85 mm, yielding a disparity of 0.35 mm (2.3%) – demonstrating good agreement
- Crack morphology: PAUT classification as planar was confirmed by metallographic examination, validating the PAUT classification approach

Root Crack (Indication 21)

- Through-wall height: PAUT measurement of 2.31 mm compared to metallographic measurement of 2.43 mm, yielding a disparity of 0.12 mm (4.9%) – demonstrating good agreement
- Root penetration: PAUT indicated slight penetration while metallography revealed moderate penetration, with the discrepancy attributed to complex root bead geometry influencing signal interpretation

- Crack morphology: PAUT classification as planar with corner trap effect was confirmed by metallographic examination, validating the PAUT classification approach

Upper Porosity (Indication 3)

- Cluster extent (width): PAUT measurement of 7.71 mm compared to metallographic measurement of 7.54 mm, yielding a disparity of 0.17 mm (2.2%) – demonstrating excellent agreement
- Cluster extent (height): PAUT measurement of 6.82 mm compared to metallographic measurement of 6.63 mm, yielding a disparity of 0.19 mm (2.8%) – demonstrating excellent agreement
- Average pore size: PAUT measurements ranging from 0.08-0.31 mm were consistent with metallographic measurements of 0.12-0.28 mm, confirming that DA^ values represent individual pore sizes for volumetric defects
- Defect morphology: PAUT classification as volumetric (porosity) was confirmed by metallographic examination, validating the PAUT classification approach

Lower Porosity (Indication 7)

- Cluster extent (height): PAUT measurement of 2.11 mm compared to metallographic measurement of 2.18 mm, yielding a disparity of 0.07 mm (3.2%) – demonstrating good agreement
- Cluster extent (width): PAUT measurement of 5.42 mm compared to metallographic measurement of 5.28 mm, yielding a disparity of 0.14 mm (2.7%) – demonstrating good agreement
- Defect morphology: PAUT classification as volumetric (porosity) was confirmed by metallographic examination, validating the PAUT classification approach

Validation Summary: Destructive metallography confirmed:

1. **ViA^ Accuracy:** Visual amplitude sizing provides accurate through-wall defect measurements for both planar and volumetric defects, with disparities <5% compared to metallographic measurements
2. **DA^ Interpretation:** Depth amplitude represents different physical quantities depending on defect type – crack height (underestimated) for toe cracks, depth location for root cracks, individual pore size for upper porosity, and depth location for lower porosity
3. **Classification Validation:** All 10 indications selected for destructive examination were correctly classified by PAUT analysis (100% classification accuracy)

DISCUSSION

Distinctive Acoustic Signatures (Research Question 1)

The analysis revealed clear and distinctive acoustic signatures for cracks and porosity in both A-scan and S-scan data. The finding that cracks produce linear S-scan patterns while porosity produces diffuse, cloud-like patterns is consistent with established PAUT literature [1, 5, 6]. Planar cracks act as specular reflectors producing distinct, well-defined echoes when the beam is oriented perpendicular to the crack face. The corner trap effect, particularly strong for root cracks, produces extremely high amplitude signals (up to 200% saturation) due to reflection from both the crack face and root geometry, a phenomenon well-documented in the literature [6, 14].

The finding that porosity produces multiple overlapping peaks in A-scan data is consistent with the physical nature of volumetric defects [5, 13]. Porosity consists of multiple small, rounded reflectors producing independent reflections. When clustered, their signals overlap, creating the characteristic complex A-scan waveform. The very small DA^ values for upper porosity (0.08-0.31 mm) are consistent with individual pore sizes, while larger ViA^ values (7.71-8.27 mm) represent overall cluster extent.

Critically, the finding that amplitude overlap occurs between cracks and porosity demonstrates that amplitude alone is not a reliable distinguishing feature. A toe crack (83.7%) overlaps with upper porosity (92.4-119.8%), and a root crack (125-200%) overlaps with lower porosity (138.2-150.2%). This challenges the common assumption that higher amplitude indicates cracks and emphasizes the need for multi-feature classification.

Sizing Accuracy Comparison (Research Question 2)

The comparison of amplitude-based sizing (DA^) with visual measurement (ViA^) revealed significant disparities. The finding that amplitude-based sizing significantly underestimates crack height (toe crack: 1.69 mm vs. 7.80 mm) is consistent with established NDT literature [2, 14, 16]. Amplitude-based sizing relies on correlation between signal amplitude and reflector size. For planar cracks, this correlation fails because: (1) amplitude depends on crack orientation relative to the beam, (2) the corner trap effect produces artificially high amplitudes, (3) signal amplitude saturates (as seen with root crack at 200%), and (4) amplitude does not correlate linearly with crack height [6, 8].

The finding that DA^ represents different physical quantities for different defect types is particularly significant. For toe cracks, DA^ represents crack height (underestimated); for root cracks, DA^ represents depth location; for upper porosity, DA^ represents individual pore size; and for lower porosity, DA^ represents depth location. This demonstrates that the same parameter cannot be interpreted uniformly without considering defect context, highlighting the need for clear interpretive guidance in PAUT inspection procedures.

The metallographic validation confirmed that ViA^ (visual amplitude) provides accurate through-wall measurements for both defect types, with disparities below 5% compared to actual measurements. This validates the use of visual spatial sizing as a reliable method when tip-diffraction measurements are not available. However, the recommended method for accurate crack sizing remains tip-diffraction, which uses time-of-flight of diffracted signals from crack tips, independent of amplitude [16]. The absence of tip-diffraction measurements in these files explains why crack sizing was inaccurate.

Classification Matrix for Distinguishing Porosity from Cracks (Research Question 3)

The classification matrix developed from this analysis provides a practical decision-support tool for PAUT inspectors. The matrix is consistent with established PAUT literature and physical principles of ultrasonic testing.

The finding that S-scan pattern and location are the most reliable distinguishing features is consistent with the literature. S-scan pattern reflects the geometry of the reflector: planar cracks produce linear, well-defined patterns due to their flat surfaces, while porosity produces diffuse, cloud-like patterns due to its multiple small reflectors. Location reflects the typical occurrence patterns of these defects in V-groove welds.

The finding that amplitude alone is not discriminatory is significant because it challenges common inspection practices. Many inspectors rely heavily on amplitude for defect characterization, assuming that higher amplitude indicates cracks. This analysis demonstrates that porosity can produce amplitudes comparable to or higher than cracks, particularly when porosity is dense or clustered. This finding emphasizes the need for multi-feature classification that combines multiple parameters.

The finding that corner trap presence is a reliable crack indicator is consistent with the literature. The corner trap effect occurs when the ultrasonic beam reflects from both the crack face and the root geometry, producing a very strong signal. This effect is particularly strong for root cracks and moderately strong for toe cracks. The absence of corner trap effect in porosity is a reliable distinguishing feature.

Based on the analysis of the PAUT data files, the following classification matrix is developed to distinguish dense, clustered porosity from planar cracks based on multi-angle PAUT beam responses.

Feature	Planar Crack (Toe)	Planar Crack (Root)	Volumetric Porosity (Upper)	Volumetric Porosity (Lower)
S-scan Pattern	Linear, well-defined	Linear, well-defined	Diffuse, cloud-like	Diffuse, cloud-like
Weld Zone	Upper Cap	Land / Root	Upper Fill	Lower Fill / near Land
Amplitude Range (A%)	80-90%	125-200% (saturated)	90-120%	138-150%
DA^ Value	Small (1.69 mm)	Large (10.27 mm)	Very small (0.08-0.31 mm)	Large (10.71-10.75 mm)
DA^ Interpretation	Crack height (underestimated)	Crack depth location	Individual pore size	Defect depth location
ViA^ Value	Large (7.80 mm)	Small (2.31 mm)	Large (7.71-8.27 mm)	Small (2.02-2.11 mm)
Indications	Single	Multiple cluster	Multiple cluster	Multiple cluster
Corner Trap Effect	Moderate	Very strong	None	None
Recommended Sizing	Tip-diffraction	Tip-diffraction	Amplitude (-6 dB)	Amplitude (-6 dB)
Confidence Level	High	High	High	High

Classification Matrix Validation

The classification matrix developed from the PAUT data analysis demonstrates that S-scan pattern and weld zone location are the most effective distinguishing features between cracks and porosity. Cracks consistently show linear, well-defined S-scan patterns, while porosity consistently shows diffuse, cloud-like patterns. The weld zone location provides additional discriminatory power: cracks are found in the Cap (toe cracks) or Land (root cracks) zones, while porosity is found in the Fill zone.

Defect Type	Indications Analyzed	Classification	Confirmed by
Toe Crack	Indication 9	Crack (Upper)	Linear S-scan, Cap zone, 83.7% amplitude
Root Crack	Indications 19-22	Crack (Lower)	Linear S-scan, Land zone, up to 200% amplitude
Upper Porosity	Indications 1-5	Porosity (Upper)	Diffuse S-scan, Fill zone, 92.4-119.8% amplitude
Lower Porosity	Indications 7-10	Porosity (Lower)	Diffuse S-scan, Lower Fill, 138.2-150.2% amplitude

Validation Accuracy: 100% for the analyzed data files (all indications correctly classified).

The amplitude behavior also provides useful classification information. Cracks exhibit corner trap effects (moderate for toe cracks, very strong for root cracks) that produce characteristic high-amplitude signals. Porosity exhibits volumetric reflections with multiple overlapping signals from individual pores. The DA^ and ViA^ values also provide useful information: for cracks, there is a significant discrepancy between DA^ and ViA^ values, while for porosity, DA^ values represent individual pores or depth location, and ViA^ values represent cluster extent.

The classification matrix is validated by the 100% correct classification of the analyzed indications. However, validation on a larger independent dataset is recommended to confirm the generalizability of the matrix.

Practical Significance of 100% Classification Accuracy

The 100% classification accuracy achieved in this study represents a significant achievement within the defined experimental scope, but this must be interpreted with careful consideration of the study's context and limitations.

Significance Within the Study Context:

The perfect classification accuracy demonstrates that, under controlled laboratory conditions with known defect types and optimized inspection parameters, PAUT combined with systematic multi-feature analysis can reliably distinguish between planar cracks and volumetric porosity. This has several important implications:

1. **Validation of Multi-Feature Approach:** The 100% accuracy validates the theoretical basis for using multiple features (S-scan pattern, weld zone location, amplitude behavior, corner trap presence, and DA/ViA relationships) rather than relying on any single parameter. This confirms that the classification matrix developed in this study is internally consistent and effective for the analyzed defect types.
2. **Methodological Framework:** The study provides a validated methodological framework that can be adapted and implemented in inspection procedures. The systematic approach of evaluating S-scan patterns first, followed by weld zone location, then amplitude behavior and corner trap presence, offers a structured decision-making process that reduces subjectivity.

3. **Training and Qualification:** The classification matrix serves as an excellent training tool for PAUT inspectors, providing clear visual and parametric criteria for distinguishing between defect types. This can help standardize interpretation and reduce variability between inspectors.

4. **Reduction of False Calls:** Accurate classification reduces both false positives (unnecessary weld repairs) and false negatives (missed critical defects). In industrial practice, the economic implications are substantial. For example, a single unnecessary weld repair on a large-diameter pipeline can cost tens of thousands of dollars in direct costs and significantly more in project delays. Conversely, a missed crack that leads to in-service failure can result in catastrophic consequences including loss of life, environmental damage, and multimillion-dollar liabilities.

Limitations Related to Specimen Diversity

Despite the 100% accuracy achieved in this study, several factors limit the generalizability of these findings to broader inspection scenarios:

1. **Limited Defect Morphologies:** The study focused exclusively on two defect types (cracks and porosity). In actual weld inspections, inspectors encounter a wider range of discontinuities including slag inclusions, lack of fusion, lack of penetration, tungsten inclusions, and complex combinations of multiple defect types. These additional defect morphologies may exhibit acoustic signatures that overlap with or mimic those of cracks and porosity, potentially reducing classification accuracy.

2. **Limited Defect Population:** The study analyzed 32 crack indications and 10 porosity indications. While sufficient for establishing baseline signatures and developing the classification matrix, this relatively small sample size limits statistical robustness. Classification accuracy of 100% on this limited dataset does not guarantee the same performance on a larger, more diverse dataset.

3. **Controlled Defect Characteristics:** The defects in this study were induced under controlled laboratory conditions. Natural or service-induced defects may have different characteristics including irregular geometries, complex branching patterns, oxide-filled cracks, or partially closed cracks that could affect acoustic response. Service-induced cracks, in particular, may have rough fracture surfaces that scatter sound differently from the relatively smooth laboratory-induced cracks used in this study.

4. **Single Material Type:** The research was conducted exclusively on structural steel (mild steel). Different materials exhibit different acoustic properties (velocity, attenuation, impedance) that can alter defect signatures. For example:

    - Austenitic stainless steel has anisotropic and coarse-grained structure causing high attenuation and beam distortion
    - Aluminum has lower velocity and higher attenuation than steel
    - Titanium has high velocity but can be noisy due to grain structure
    - Dissimilar metal welds create complex impedance boundaries

5. **Single Weld Geometry:** The study used a single V-groove butt weld configuration with 9.50 mm thickness. Different weld geometries (single-bevel, double-bevel, narrow-gap, T-joints, pipe welds) create different geometric reflections and may affect how defects present in PAUT images.

6. **Ideal Surface Conditions:** The laboratory specimens had ideal surface conditions with good acoustic coupling. Field inspections often encounter surface roughness, corrosion, paint, or limited access that degrade signal quality and may obscure distinguishing features.

Limitations Related to Field Applicability

Translating laboratory findings to field inspection practice presents several challenges:

1. **Environmental Factors:** Field inspections occur under challenging conditions including temperature variations (which affect sound velocity), humidity, dust, and vibration. These factors can degrade signal quality, increase noise levels, and affect calibration stability.

2. **Access Restrictions:** Welds in service are often in confined spaces, at heights, or in hazardous environments that restrict probe positioning and scanning patterns. The optimized scanning configuration used in this study may not be achievable in all field situations.

3. **Surface Preparation:** Laboratory specimens were prepared with smooth surfaces for optimal coupling. In the field, welds may have surface irregularities, weld reinforcement, or coating that affect coupling and signal quality.

4. **Complex Geometry:** Field welds may have more complex geometries than the simple V-groove used in this study. Complex geometries create additional geometric reflections and shadowing that can obscure defect signals.

5. **Operator Variability:** PAUT interpretation remains highly operator-dependent despite advanced software tools. Different inspectors may apply the classification matrix differently, use slightly different cursor placements, or have varying levels of experience in identifying distinguishing features.

6. **Calibration Stability:** Field conditions can cause calibration drift over time, affecting amplitude measurements and positional accuracy. Maintaining calibration stability over extended inspection periods is challenging.

7. **Multiple Defects:** Field inspections often encounter multiple defects in the same weld zone, creating complex overlapping signals that may be difficult to interpret using the classification matrix.

Recommendations for Field Implementation

Given these limitations, the following recommendations are made for implementing the classification matrix in field inspections:

1. **Use as Decision-Support Tool:** The classification matrix should be used as a decision-support tool rather than a rigid rule. Inspectors should consider multiple features and exercise professional judgment, particularly when features are not clearly defined.

2. **Consider Confidence Levels:** When applying the matrix, inspectors should document confidence levels based on how clearly the distinguishing features are observed. Low-confidence classifications should trigger additional investigation or conservative acceptance criteria.

3. **Complement with Other NDT Methods:** When classification is ambiguous, consideration should be given to using complementary NDT methods such as radiography, magnetic particle inspection, or time-of-flight diffraction (TOFD) to confirm the classification.

4. **Field Validation:** Before adopting the classification matrix for a specific application, field validation should be conducted on representative specimens or through destructive testing of representative samples.

5. **Training and Qualification:** Inspectors applying the classification matrix should receive specific training on the criteria and should demonstrate proficiency on known reference specimens.

ISSN No. 2321-2705 | DOI: 10.51244/IJRSI |Volume XIII Issue VI June 2026

6. **Documentation:** All classification decisions should be documented, including the reasoning behind the classification and any uncertainties or limitations encountered.

Statistical Performance Considerations

While the classification matrix achieved 100% accuracy on the analyzed dataset, several statistical considerations should be addressed in future research:

1. **Sensitivity and Specificity:** On the limited dataset (32 crack indications, 10 porosity indications), sensitivity (true positive rate for cracks) would be 100% and specificity (true negative rate, correctly identifying porosity as non-crack) would also be 100%. However, these perfect metrics are likely inflated due to the small sample size and controlled conditions.

2. **Confusion Matrix:** A confusion matrix for this dataset would show no misclassifications, but this should not be interpreted as evidence that misclassifications will not occur in practice. With larger, more diverse datasets, some confusion between defect types is expected.

3. **Confidence Intervals:** With only 42 total indications, confidence intervals around the 100% accuracy estimate would be wide. The Wilson score interval for 42 observations with zero failures gives a 95% confidence interval of approximately 91.5% to 100%. This suggests that while the accuracy is high, the lower bound of 91.5% indicates that some misclassifications may occur in practice.

4. **Sample Size Requirements:** For robust statistical validation, future studies should aim for larger sample sizes (minimum 50-100 indications per defect type) with independent validation datasets not used for matrix development.

Comparison with Literature

The findings of this study are broadly consistent with previous research on PAUT defect characterization [1, 5, 6, 8, 14]. The distinctive acoustic signatures for cracks and porosity have been previously described, and the limitations of amplitude-based sizing for planar cracks are well-established. However, this study makes several novel contributions:

1. **Systematic Classification Matrix:** While individual distinguishing features have been described, this study provides a systematic, multi-feature classification matrix with explicit criteria and validation.

2. **Quantitative Thresholds:** The study provides quantitative ranges for distinguishing features (amplitude ranges, DA^ values, ViA^ values) that can be used as practical guidelines.

3. **Parametric Interpretation Guidance:** The study clarifies that the same parameter (DA^) has different physical meanings for different defect types, providing clear interpretive guidance.

4. **Validation with Destructive Metallography:** The destructive metallographic validation provides strong empirical support for the classification matrix.

5. **Comprehensive Sizing Guidance:** The study provides clear guidance on appropriate sizing methods for different defect types based on validation results.

Recommendations for Future Research

Based on the findings and limitations of this study, several directions for future research are recommended:

1. **Extended Validation:** The classification matrix should be validated on larger, independent datasets including different materials, weld geometries, and defect types.

2. **Field Validation Studies:** The matrix should be tested in field inspection conditions to assess its performance under realistic operating conditions.

3. **Statistical Performance Assessment:** Future studies should report sensitivity, specificity, and confusion matrices to provide more robust performance metrics.

4. **Machine Learning Applications:** The classification matrix could be used as a basis for developing machine learning algorithms for automated defect classification.

5. **Advanced PAUT Techniques:** The effectiveness of the classification matrix should be evaluated when using advanced PAUT techniques such as Full Matrix Capture (FMC), Total Focusing Method (TFM), or Phase Coherence Imaging (PCI).

6. **Multi-Operator Studies:** The inter-operator reliability of the classification matrix should be assessed through multi-operator studies.

7. **Natural Defects:** The study should be extended to include naturally occurring or service-induced defects to assess whether acoustic signatures differ under real-world conditions.

CONCLUSION

This study has demonstrated that cracks and porosity exhibit distinctive acoustic signatures in PAUT A-scan and S-scan data, that amplitude-based sizing is unreliable for cracks while appropriate for porosity, and that a classification matrix based on S-scan pattern, location, amplitude behavior, and DA/ViA relationships can effectively distinguish these defect types. The key recommendations derived from this research emphasize the need for tip-diffraction application for crack sizing, systematic -6 dB drop method for porosity boundaries, and the implementation of the classification matrix as a decision-support tool. Training programs must address the gap between recommended and actual practice, and procedures and standards should be updated to reflect these findings. By implementing these recommendations, inspectors can make more accurate decisions regarding weld acceptance or rejection, improving the safety, reliability, and cost-effectiveness of welded structures across industries. Future research should continue to validate and refine these findings, expand the scope of investigation, and develop automated tools for defect classification and sizing.

FINDINGS

The analysis of the PAUT data files confirms the three research hypotheses:

1. **Distinctive Acoustic Signatures:** Cracks and porosity exhibit clearly distinguishable acoustic signatures in both A-scan and S-scan data. Cracks produce linear S-scan patterns with sharp A-scan signals and corner trap effects. Porosity produces diffuse S-scan patterns with multiple overlapping A-scan signals and no corner trap effect.

2. **Sizing Accuracy Comparison:** Amplitude-based sizing is unreliable for cracks, significantly underestimating crack height (toe crack: 1.69 mm vs 7.80 mm) or becoming impossible due to signal saturation (root crack: 200%). Amplitude-based sizing is appropriate for porosity when applied correctly (measuring individual pores or applying -6 dB drop for cluster boundaries). Tip-diffraction is the recommended method for accurate crack sizing but was not applied in these files.

3. **Classification Matrix:** A classification matrix based on S-scan pattern, weld zone location, amplitude behavior, and DA^/ViA^ values can effectively distinguish dense, clustered porosity from planar cracks. The matrix achieved 100% classification accuracy for the analyzed data files, providing a practical decision-support tool for PAUT inspectors.

The findings provide empirical evidence supporting the research objectives and contribute to improved PAUT weld defect characterization practice. The classification matrix and sizing guidance developed from this analysis can help inspectors make more accurate decisions regarding weld acceptance or rejection, improving the safety and reliability of welded structures.

Future Research Directions

The future research directions will collectively contribute to improved PAUT weld defect characterization practice, enhancing the safety, reliability, and cost-effectiveness of welded structures across industries. The ultimate goal is to develop a comprehensive, validated framework for PAUT defect characterization that is robust across materials, geometries, and inspection conditions, and that can be implemented reliably by inspectors at all skill levels.

RECOMMENDATION

PAUT systems should be configured to optimize tip-diffraction signal detection, with appropriate gain settings, filtering, and display configurations that make tip signals visible and measurable. The digitizing frequency of 100 MHz used in this research provides 0.016 mm depth resolution, which is sufficient for precise tip-diffraction measurements and should be maintained. Video filter should be on to smooth the display and facilitate tip identification, while rectification should be set to full wave to preserve signal morphology. Gain settings should be adjusted to avoid saturation, particularly for root cracks where the corner trap effect can produce extremely high amplitudes. Encoder resolution of 12 steps/mm provides positional accuracy of 0.083 mm and should be maintained for precise defect location mapping.

ACKNOWLEDGMENTS

The authors acknowledge the support of METIRDC for providing access to inspection data and facilities. The contributions of the study team in conducting inspections are gratefully recognized. The authors also thank relevant staffs for administrative support.

Funding Statement

This research was supported by the Manufacturing Industry Development Institute (MIDI), Addis Ababa, Ethiopia, under NDT laboratory researcher team. The funding agency provided access to inspection equipment and testing facilities but had no role in study design, data collection, analysis, interpretation, or manuscript preparation.

Author Contributions: Nardos Mekoya conceived and designed the study, analyzed data, and wrote the manuscript. Technical analysis. Dejene Legesse, data collection and interpretation, reviewed the manuscript.

Conflicts of Interest: The authors declare no conflicts of interest.

Data Availability: The data supporting the findings of this study include Omni PC scan files. Due to the proprietary nature of the software data formats and specific industrial sample configurations, the datasets are not publicly deposited. However, the corresponding author can provide access to the raw data upon reasonable request.

Data Availability Statement

The Omni PC scan files generated during this study are not publicly available due to the proprietary nature of the software data formats and specific industrial sample configurations. However, the author (Nardos Mekoya, mekoyan82@gmail.com) can provide access to the raw data in a standardized format upon reasonable request from qualified researchers, subject to institutional data access policies. All processed data presented in this manuscript are included in the tables and figures.

Ethics Statement: This study involved analysis of existing inspection data and did not involve human subjects or animal studies. All data analysis was conducted in accordance with established research ethics guidelines.

REFERENCES

1. Bridge, B. (2019). Advanced Ultrasonic Testing Techniques for Industrial Weld Inspections. London: Academic Press.
2. Silk, M. G. (2016). Ultrasonic Transducers for Nondestructive Testing. Bristol: Adam Hilger Publishing.
3. Drinkwater, B. W., & Wilcox, P. D. (2006). Ultrasonic phased arrays: A review. NDT & E International, 39(7), 525-541.
4. Clay, A. C., Wooh, S. C., Azar, L., & Wang, J. Y. (1999). Experimental evaluation of phased array ultrasonic technology for weld inspection. Journal of Nondestructive Evaluation, 18(2), 59-71.
5. Olympus-NDT. (2022). Phased Array Testing: Technology and Equipment Applications Guide. Waltham, MA: Evident Scientific.
6. Krautkrämer, J., & Krautkrämer, H. (1990). Ultrasonic Testing of Materials (4th ed.). Berlin: Springer-Verlag.
7. Ogilvy, J. A. (1989). Model for the ultrasonic inspection of rough defects. Ultrasonics, 27(4), 194-209.
8. Langenberg, K. J., Marklein, R., & Mayer, K. (2012). Advanced Electromagnetism and Acoustics: Foundations and Computer Applications. Boca Raton: CRC Press.
9. ASME International. (2023). ASME Boiler and Pressure Vessel Code, Section V: Nondestructive Examination, Article 4: Ultrasonic Examination Methods for Welds. New York: The American Society of Mechanical Engineers.
10. American Welding Society. (2020). AWS D1.1/D1.1M: Structural Welding Code – Steel. Miami, FL: American Welding Society.
11. Moles, M. (2014). Selecting Software-Assisted Post-Processing Parameters for Advanced PAUT Analysis. Toronto: NDT Media Publishing